The Astrophysical Journal Letters, 737:L4 (6pp), 2011 August 10 doi:10.1088/2041-8205/737/1/L4

SPECTROSCOPIC OBSERVATIONS OF A CORONAL MORETON WAVE

Louise K. Harra[1], Alphonse C. Sterling[2,5], Peter Gömöry[3], and Astrid Veronig[4]
[1] UCL-Mullard Space Science Laboratory, Holmbury St. Mary, Dorking, Surrey, RH5 6NT, UK; lkh@mssl.ucl.ac.uk
[2] Space Science Office, VP62, NASA Marshall Space Flight Center, Huntsville, AL 35812, USA; alphonse.sterling@nasa.gov
[3] Astronomical Institute, Slovak Academy of Sciences, SK-05960 Tatranská Lomnica, Slovakia; gomory@astro.sk
[4] Institute of Physics, University of Graz, Universitätsplatz 5, A-8010 Graz, Austria; astrid.veronig@uni-graz.at
Received 2011 May 17; accepted 2011 July 1; published 2011 July 15

ABSTRACT

We observed a coronal wave (EIT wave) on 2011 February 16, using EUV imaging data from the *Solar Dynamics Observatory*/Atmospheric Imaging Assembly (AIA) and EUV spectral data from the *Hinode*/EUV Imaging Spectrometer (EIS). The wave accompanied an M1.6 flare that produced a surge and a coronal mass ejection (CME). EIS data of the wave show a prominent redshifted signature indicating line-of-sight velocities of ∼20 km s^{-1} or greater. Following the main redshifted wave front, there is a low-velocity period (and perhaps slightly blueshifted), followed by a second redshift somewhat weaker than the first; this progression may be due to oscillations of the EUV atmosphere set in motion by the initial wave front, although alternative explanations may be possible. Along the direction of the EIS slit the wave front's velocity was ∼500 km s^{-1}, consistent with its apparent propagation velocity projected against the solar disk as measured in the AIA images, and the second redshifted feature had propagation velocities between ∼200 and 500 km s^{-1}. These findings are consistent with the observed wave being generated by the outgoing CME, as in the scenario for the classic Moreton wave. This type of detailed spectral study of coronal waves has hitherto been a challenge, but is now possible due to the availability of concurrent AIA and EIS data.

Key words: Sun: coronal mass ejections (CMEs)

Online-only material: animation

1. INTRODUCTION

The nature of large-scale waves in the corona has been debated for many years. Attention was alerted to the phenomena in the 1960s when global waves were observed in the chromosphere in Hα (e.g., Moreton & Ramsey 1960; Athay & Moreton 1961). The waves became known as "Moreton waves" and have speeds of propagation of the order of 1000 km s^{-1}. These waves were found to be too fast to originate in the chromosphere. Uchida (1968) developed a theory of the fast-mode MHD shock wave where the wave radiated out into the corona from a flare site and energy is refracted down into the chromosphere. There is a down-up swing observed in the chromospheric Hα line which is explained by a depression in the chromosphere caused by the coronal shock followed by a relaxation (see a recent review on flares by Hudson 2011). The problem is that the coronal counterpart of the Moreton wave is difficult to observe.

When the phenomena of "EIT waves" were first discovered in the late 1990s, it was initially thought that these were the coronal Moreton waves as described by Uchida (1968). The EUV Imaging Telescope (Delaboudinière et al. 1995) on board *SOHO* made observations of a diffuse propagating bright front reaching speeds of several hundred km s^{-1} (Thompson et al. 1998). Since their discovery the explanation of EIT waves has developed with several hypotheses put forward. These can be simply split into wave and non-wave phenomena. Evidence for waves includes similar kinematical curves across a broad range of wavelengths with waves in all wavelengths decelerating (Warmuth et al. 2004), waves seen to reflect off coronal holes (e.g., Gopalswamy et al. 2009b; evidence for a fast-mode MHD wave initiated by a coronal mass ejection (CME; Kienreich et al. 2009) and evidence of a dome-shaped structure that expands laterally much further than dimming is observed (Veronig et al. 2010)). The non-wave explanations are based around the propagation of the CME and its interaction with its surroundings (e.g., Zhukov et al. 2009; Attrill et al. 2007; Delannèe et al. 2008; Ma et al. 2009). Hybrid explanations that combine both CME propagation and wave aspects have been described by Chen et al. (2005) and Liu et al. (2010). We refer the reader to two excellent reviews that describe EIT waves in more detail: Wills-Davey & Attrill (2009) and Gallagher & Long (2010).

There have been few spectroscopic observations of EIT waves in the corona. The first by Harra & Sterling (2003) studied a wave on 1998 June 13 which was observed by the *TRACE* spacecraft and the Coronal Diagnostic Spectrometer (CDS) on board *SOHO*. There were two waves observed in *TRACE*—one had the typical bright front with a speed of 200 km s^{-1} and the second was faster with a speed of 500 km s^{-1} but weaker. The weak wave showed no spectroscopic signature as it propagated through the CDS field of view (FOV). This could be because there were no strong velocities, i.e., $v < 10$ km s^{-1}, the emission measure was too low to be measured, or there simply were no Doppler shifts. The strong wave shows a high line-of-sight velocity feature in the transition region which corresponds to the erupting filament material. These observations are consistent with the numerical simulations of the hybrid model of Chen et al. (2005) which shows both a fast-mode MHD wave and the opening up of field lines due to the erupting filament. Another example of spectroscopic observations was from a large X-class flare observed soon after the launch of the *Hinode* spacecraft. In that event Asai et al. (2008) found two separate blueshifted phenomena observed by the EUV Imaging Spectrometer (EIS). The first was related to a plasmoid ejection and was observed in

[5] Current address: JAXA/Institute of Space and Astronautical Science, Hinode Group, 3-1-1 Yoshinodai, Sagamihara, Chuo-ku, Kanagawa 252-5210, Japan.

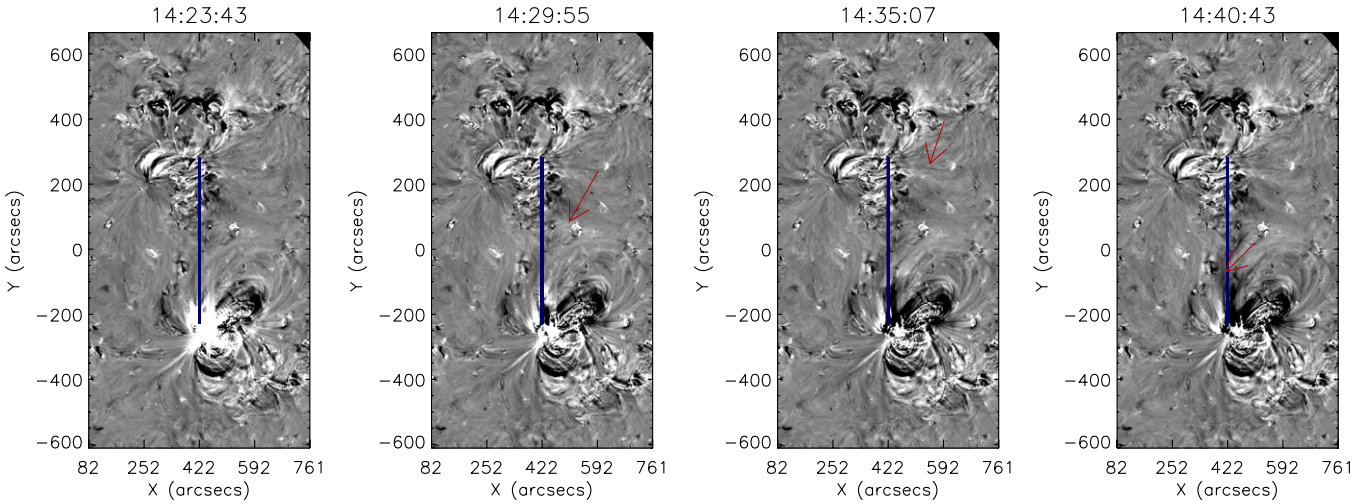

Figure 1. Base difference images derived from AIA 193 Å passband data showing the time period when the two wave fronts passed through the EIS field of view. The base image subtracted from the others was at 13:01 UT. The position of the EIS slit is marked as a blue solid vertical line. Red arrows in frames 2 and 3 highlight the wave front and in frame 4 the surge is highlighted.

(An animation of this figure is available in the online journal.)

all the emission lines. The second was related to an arc-shaped propagating structure seen in X-rays and was only observed in the hotter emission lines in the EIS study. They were found close to the flaring active region. Chen et al. (2010) also studied the behavior of the Doppler shifts and line widths of an EIT wave. They found the classic features of outflowing plasma in the dimming region seen behind the EIT wave (e.g., Harra & Sterling 2001). In addition, they found a second blueshifted component of 100 km s^{-1} with a drift velocity along the slit of 450 km s^{-1} only observed in Fe XV and Ca XVII which corresponded to the shock wave associated with the flare. These observations were also close to the flaring active region.

In this Letter, using data from Atmospheric Imaging Assembly (AIA) and EIS we analyze an "EIT wave" of 2011 February 16 as it propagates north of active region 11158, the source region of the eruption, toward active region 11159. The EIS slit was lying between the two active regions allowing us to determine for the first time with a high time cadence the spectroscopic signature of an EIT wave in the corona as it propagates away from the active region.

2. OBSERVATIONS

The EIS on board *Hinode* (Culhane et al. 2007) is a scanning slit spectrometer observing in two wave bands in the EUV: 170–210 Å and 250–290 Å. The spectral resolution is 0.0223 Å $pixel^{-1}$, which allows velocity measurements of a few km s^{-1}. The temperature coverage ranges from log T = 4.7–7.3 with a spatial resolution of close to 1″–2″. The data in this study were acquired during campaign HOP180[6] performed during 2011 February 10–17. HOP180 was specifically designed to study plasma diagnostics, plasma flows, and their dynamics at EIT wave fronts by combining high-cadence sit-and-stare EIS spectroscopy in various chromospheric, transition region and coronal spectral lines with high-cadence multiwavelength imaging by AIA. For this observation, the 2″ slit was used in "sit-and-stare" mode between active regions 11158 and 11159. The slit height was 512″ (with a pixel size of 1″ in the y-direction) and an exposure time of 45 s. We concentrate on the observations starting at 14:08 UT and focus on the Fe XII 195.12 Å (log T = 6.1) and the Fe XIII 202.04 Å (log T = 6.2) spectral windows. We fitted the data using a single Gaussian in most cases, but applied a double-Gaussian fit in the region closest to the eruption, where two components are clearly seen.

The AIA on board the *Solar Dynamics Observatory* (*SDO*) has a spatial resolution of 1.″4 and a high time cadence. For this sequence we used a subset of AIA images which gave a cadence of 25 s. For the analysis we concentrated on the 193 Å bandpass as the wave is seen most clearly in this band. It is also the passband that includes the EIS 195 Å emission line.

Figure 1 presents base difference images from AIA. The images were de-rotated, and then the first image in the sequence was subtracted from the subsequent images. The M1.6 flare started at 14:19 UT in AR 11158 (the southern active region). The flare was impulsive, peaking five minutes later. The flare itself was over in less than 40 minutes, so was not a long-duration event, but nonetheless images from EUV and coronagraph instruments on *STEREO* show a clear ejection and CME. The first image shown in Figure 1 shows the intense brightening of the flare, just before the peak was reached. The second image shows a weak wave front approaching the northern active region. The third image shows a dimming region firmly established north of the flaring active region. Finally, another weak wave front passes through. Arrows highlight the first wave propagating, and then the surge. From the AIA images we estimate the speed of the first wave to be 500 ± 50 km s^{-1}. This all happened in only 17 minutes and would have been very difficult to see with *SOHO* EIT due to the lower time cadence. The wave fronts are very weak and more easily seen in the animation available in the online version of the journal.

Figure 2 shows EIS Fe XII intensity data. Since this is a sit-and-stare study the morphology is difficult to track. The FOV is shown in Figure 1. The lower part of the EIS FOV lies on the southern active region. In this region very strong outflows are seen, illustrated by the strong blueshifted secondary components in the line profiles. These speeds reach over 400 km s^{-1}—indeed the secondary component is so fast that it falls out of the EIS spectral window in some cases. For values from y = −130″ increasing in the y-direction between about 14:23UT and 14:30 UT, there is an extremely weak feature in the intensity

[6] HOP 180 PIs: P. Gömöry, A. Veronig; for details see http://www.isas.jaxa.jp/home/solar/hinode_op/hop.php?hop=0180.

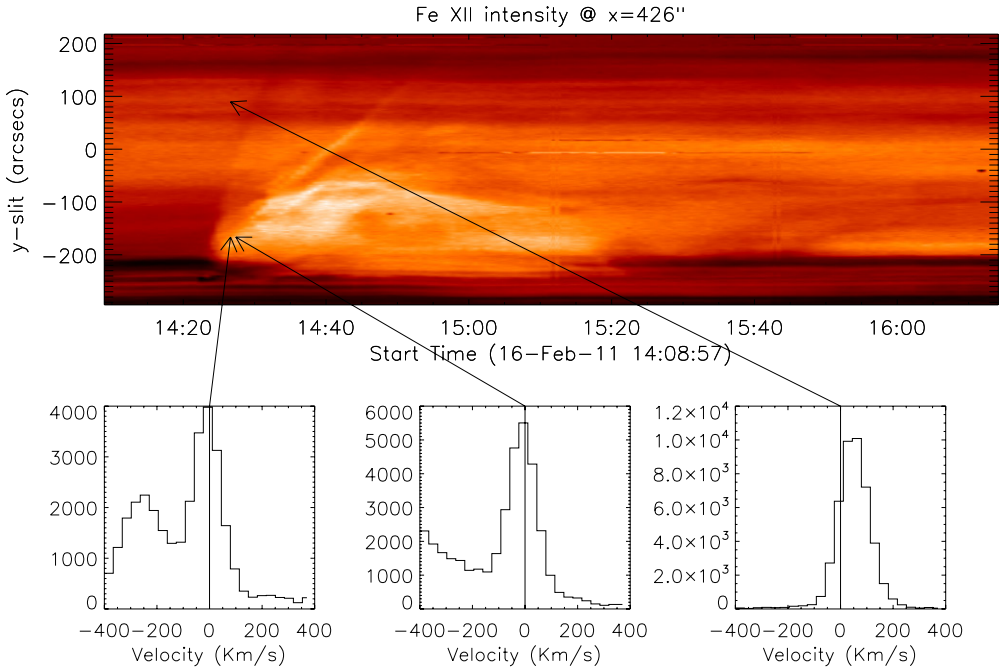

Figure 2. Top image shows the time evolution of the EIS Fe XII intensity, where the *y*-axis shows the position along the slit in arcsecs at the *x* position of 426″ (cf. Figure 1). The three lower figures show sample spectra at different positions. The first two spectra show a strongly blueshifted component at the eruption site, reaching speeds of over 400 km s^{-1}. The right-hand plot shows a spectrum at the position of the first wave front. The black vertical lines on the spectral plots show the position of zero velocity. The arrows show the pixel location for each spectrum with redshift and blueshift corresponding to positive and negative velocities, respectively.

that is not clearly seen. However, the spectral profile at this point shows a clear Doppler redshift.

To study this weak-intensity feature in more detail, we look at the Doppler velocity images and the line width images with time. Figure 3 shows this, along with the Fe XIII intensity image. A strong blueshifted component occurs near the flare site (marked as "feature 1" in Figure 3). This blueshift evolves into a predominately redshift from about 14:45 UT. This feature corresponds to a surge-like feature, visible in AIA movies (cf. Figure 1, panel 4), that flows upward along magnetic loops from AR 11158 toward AR 11159, and then largely retreats (falls) along the same loop fields toward AR 11158. Rapidly speeding away from this surge feature is a wave front (marked as "feature 2") that has a prominent redshifted component with a line-of-sight velocity of ∼20 km s^{-1}, and a speed of propagation along the direction of the EIS slit of around 510 km s^{-1}, which is consistent with the estimate obtained from the AIA difference images. A second redshifted propagation occurs later (marked as "feature 3"), which is extended over time and hence has a range of propagation speeds of between 200 and 500 km s^{-1}. Figure 3 shows the positions of the redshifted features, blueshifted features, and intensity enhancements to be in different locations. We explore this by looking at slices at different *y* positions.

This second wave front has an intensity enhancement lagging it, as can be seen from the overlying contours in Figure 3. We will consider the possible nature of this second wave in the discussion section.

Figure 4 shows two slices of the intensity, Doppler velocity, and line width for the Fe XII ion. We choose $y = 0''$ and $y = 100''$ to catch the waves as they propagated without contamination from the active region itself. The intensity does not show very strong change—a small dimming is seen at 14:40 at $y = 0''$, and some other variations. The Doppler velocity plot shows more pronounced details. At $y = 0''$, there is a clear redshift at about 14:27, and a redshift more broadly dispersed in time over about 14:35 to 14:39, with a slower velocity period at around 14:30 UT. At $y = 100''$, there is a larger sharply peaked redshift near 14:29, followed by a sharp drop in velocity (with minimum near 14:35 UT) and then another strong redshift around 14:40. The $y = 0''$ sharp blueshift at 14:42 is almost certainly from the surge material (feature 1 of Figure 3).

Figure 5 shows the same information for the Fe XIII ion. The intensity enhancement related to the first wave front is seen clearly this time, at 14:31 at $y = 100''$. This has an associated redshift of 20 km s^{-1}. The second redshift component is then seen related to the second wave front, with an intensity increase broader in time than that of the first redshift. The peaks related to the wave fronts are marked with red arrows in Figure 5. For both Fe XII (Figure 4) and Fe XIII (Figure 5), the line width increases at the same times that the redshift becomes enhanced.

3. DISCUSSION

By combining data from AIA and EIS, we are able to examine a coronal wave with high cadence and spectral detail, something that was extremely challenging prior to the *Hinode* and *SDO* era. We find that the main wave front travels at ∼500 km s^{-1} and is strongly redshifted (i.e., as the wave propagates it also pushes plasma downward toward the Sun with a speed of ∼20 km s^{-1}). This main wave front is followed by a low-velocity (near zero km s^{-1}) period, and then a second redshifted feature that has a range of velocities between 200 and 500 km s^{-1} and of comparable or somewhat lower Doppler velocity.

Uchida (1968) suggested that a Moreton wave forms when a coronal MHD shock propagating away from a source region, pushes down the chromospheric plasma along the shock front. Our observations of prominent redshifts corresponding to the intensity wave front of an EIT wave observed in AIA are

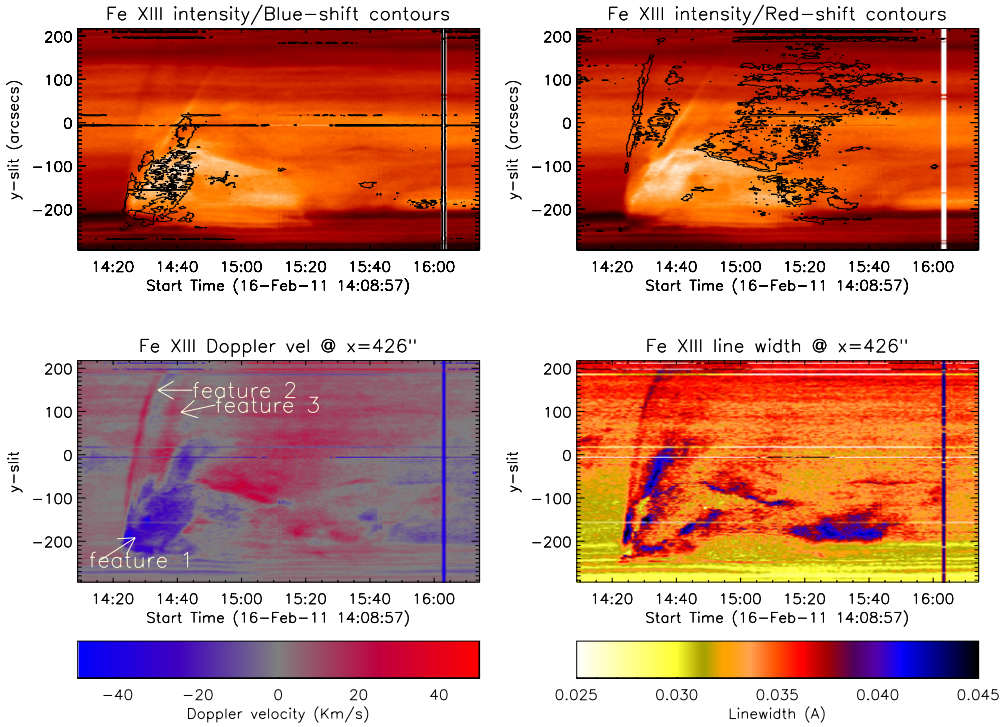

Figure 3. Top left image is the EIS Fe XIII intensity with time. The contours highlight the regions with blueshifted plasma. The top right image is the EIS Fe XIII intensity with time. The contours highlight the redshifted plasma. The bottom left image shows the Doppler velocity of Fe XIII with time, ranging between +/− 50 km s^{-1}. The bottom right image shows the line width of the Fe XIII ion with time. There is an artifact in the data at 16:00.

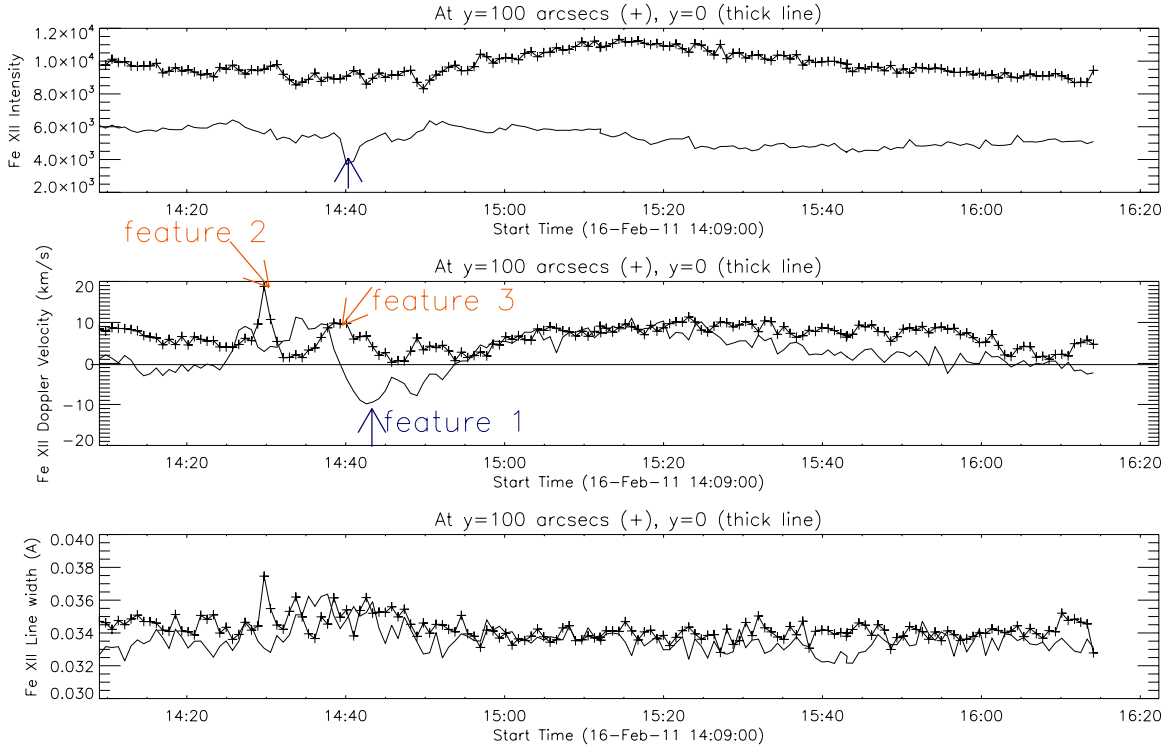

Figure 4. Top panel shows the variation of intensity with time for the Fe XII ion at $y = 100''$ and at $y = 0''$. The middle panel shows the temporal variation of the Fe XII Doppler velocity at $y = 100''$ and $y = 0''$, where redshift and blueshift are positive and negative velocities, respectively. The bottom panel shows temporal variation of the Fe XII line width at $y = 0''$ and $y = 100''$.

consistent with the EIT wave having characteristics analogous to a Moreton wave in the EUV solar atmosphere.

The origin of the second redshifted feature (feature 3 in Figure 3) is less clear. It is possibly an extended response of the low atmosphere to the initial depression from the hydrodynamic disturbance making the wave front, that is, a down–up swing of the atmosphere. In such a case it is not obvious why the second wave would have a reduced velocity over that of the wave front

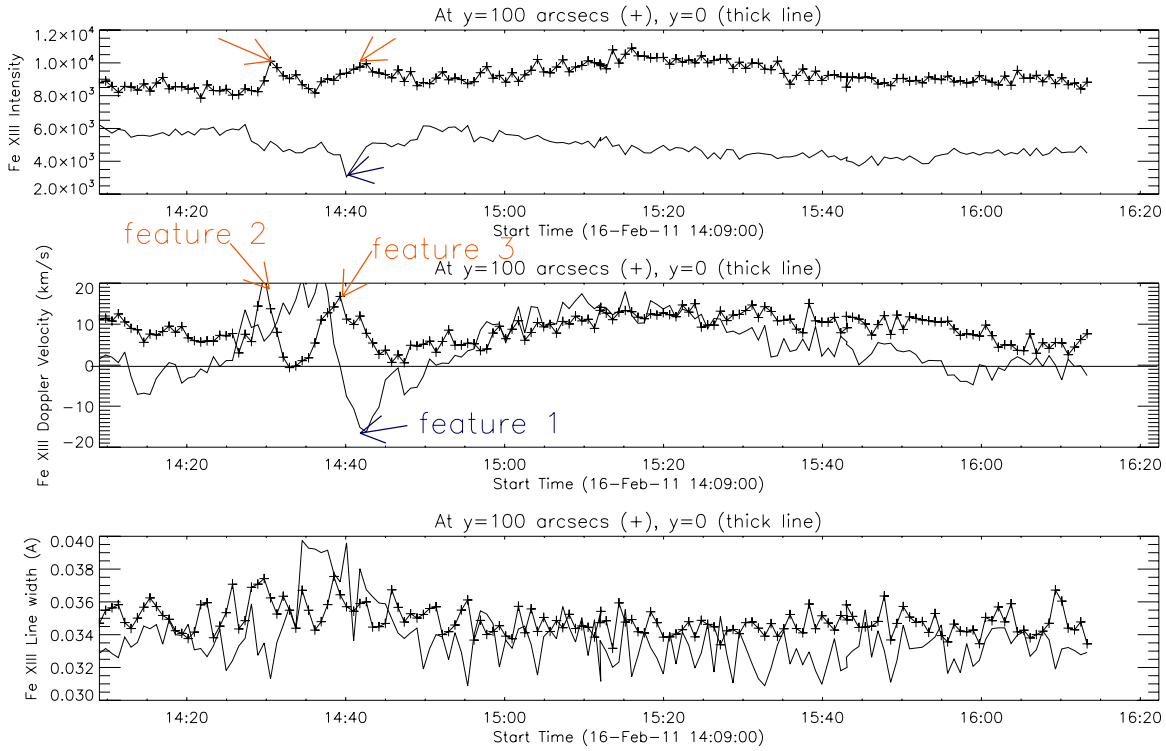

Figure 5. Top panel shows the variation of intensity with time for the Fe XIII ion at $y = 100''$ and at $y = 0''$. The middle panel shows the temporal variation of the Fe XIII Doppler velocity at $y = 100''$ and $y = 0''$, where redshift and blueshift are positive and negative velocities, respectively. The bottom panel shows temporal variation of the Fe XIII line width at $y = 0''$ and $y = 100''$. The red arrows highlight features related to the wave front and the blue arrows those related to the surge.

and that the blueshifted features are extremely weak (if they exist at all). Other possibilities for the second wave include wave oscillations generated by the wave while it propagates as predicted by Chen et al. (2002), some aspects of the CME perhaps generating a backward push on the lower atmosphere as the CME expands while moving outward, or that the signature may result from a downward-directed seemingly faster-moving portion of the surge which we see in AIA 304 Å movies that traverse the magnetic loops between the two active regions. Independent of how it is produced, this feature may be similar to secondary wave components observed by Harra & Sterling (2003) and Liu et al. (2010), and therefore this may be a common aspect of EIT waves. These preliminary results cannot identify this clearly and more detailed analysis and perhaps observations of similar events is required.

If our wave front is due to an MHD fast-mode shock wave as envisioned by Uchida (1968), then we might expect a signature of the event in solar radio data. NOAA records show that there was a Type II radio burst over 2011 February 16 14:23 UT–14:35 UT, and a Type IV burst over 14:31 UT–16:13 UT. Type II bursts are from the propagation of shocks in the heliosphere, while many Type IVs result from electrons trapped in the flaring region (e.g., Caroubalos et al. 2004; Gopalswamy et al. 2005, 2009a).

Not all EIT waves are necessarily as we describe here, and others may represent different phenomena (Wills-Davey & Attrill 2009; Hudson 2011). More joint studies using AIA, EIS, and other instruments are needed to better elucidate the properties of this phenomenon.

We are grateful to the anonymous referee for helping us improve the clarity of the Letter. We thank R. L. Moore and N. Gopalswamy for helpful discussions. A.C.S. was supported by NASA's Science Mission Directorate through the LWS TR&T and the Solar Physics Supporting Research and Technology programs. *Hinode* is a Japanese mission developed and launched by ISAS/JAXA, collaborating with NAOJ as a domestic partner and NASA and STFC (UK) as international partners. Scientific operation of the *Hinode* mission is conducted by the *Hinode* science team organized at ISAS/JAXA. This team mainly consists of scientists from institutes in the partner countries. Support for the post-launch operation is provided by JAXA and NAOJ (Japan), STFC (UK), NASA (USA), ESA, and NSC (Norway). A.V. acknowledges the Austrian Science Fund (FWF): P20867-N16. P.G. acknowledges the support of the VEGA grant 2/0064/09.

REFERENCES

Asai, A., Hara, H., Watanabe, T., et al. 2008, ApJ, 685, 622
Athay, R. G., & Moreton, G. E. 1961, ApJ, 133, 935
Attrill, G. D. R., Harra, L. K., van Driel-Gesztelyi, L., & Démoulin, P. 2007, ApJ, 656, L101
Caroubalos, C., Hillaris, A., Bouratzis, C., et al. 2004, A&A, 413, 1125
Chen, F., Ding, M. D., & Chen, P. F. 2010, ApJ, 720, 1254
Chen, P. F., Fang, C., & Shibata, K. 2005, ApJ, 622, 1202
Chen, P. F., Wu, S. T., Shibata, K., & Fang, C. 2002, ApJ, 572, L99
Culhane, J. L., Harra, L. K., James, A. M., et al. 2007, Sol. Phys., 243, 19
Delaboudinière, J.-P., Artzner, G. E., et al. 1995, Sol. Phys., 162, 291
Delannèe, C., Török, T., Aulanier, G., & Hochedez, J.-F. 1995, Sol. Phys., 162, 291
Gallagher, P. T., & Long, D. M. 2010, Space Sci. Rev.
Gopalswamy, N., Aguilar-Rodriguez, E., Yashiro, S., et al. 2005, J. Geophys. Res., 110, A12S07
Gopalswamy, N., Thompson, W. T., Davila, J. M., et al. 2009a, Solar Phys., 259, 227
Gopalswamy, N., Yashiro, S., Temmer, M., et al. 2009b, ApJ, 691, L123
Harra, L. K., & Sterling, A. C. 2001, ApJ, 561, 215
Harra, L. K., & Sterling, A. C. 2003, ApJ, 587, 429
Hudson, H. S. 2011, Space Sci. Rev., 158, 5

Kienreich, I. W., Temmer, M., & Veronig, A. 2009, ApJ, 703, L118
Liu, W., Nitta, N. V., Schrijver, C. J., Title, A. M., & Tarbell, T. D. 2010, ApJ, 723, L53
Ma, S., Wills-Davey, M. J., Lin, J., et al. 2009, ApJ, 707, 503
Moreton, G. E., & Ramsey, H. E. 1960, PASP, 72, 357
Thompson, B. J., Plunkett, S. P., Gurman, J. B., et al. 1998, Geophys. Res. Lett., 25, 2465
Uchida, Y. 1968, Sol. Phys., 4, 30
Veronig, A., Muhr, N., Kienreich, I. W., Temmer, M., & Vršnak, B. 2010, ApJ, 716, L57
Warmuth, A., Vršnak, B., Magdalenić, J., Hanslmeier, A., & Otruba, W. 2004, A&A, 418, 1101
Wills-Davey, M. J., & Attrill, G. D. R. 2009, Space Sci. Rev., 149, 325
Zhukov, A. N., Rodriguez, L., & de Patoul, J. 2009, Sol. Phys., 259, 73